Electronic Supplementary Information for:

Harnessing the power of thermoplastic elastomer-derived ordered mesoporous carbons through functionalization

Mark Robertson[1], Andrew Barbour[1], Anthony Griffin[1], Jeffrey Aguinaga[1], Derek Patton[1], Yizhi Xiang[2], Zhe Qiang[1,]*

[1]School of Polymer Science and Engineering, University of Southern Mississippi, Hattiesburg, Mississippi, 39406, USA

[2]Dave C. Swalm School of Chemical Engineering, Mississippi State University, Mississippi State, Mississippi, 39762, USA

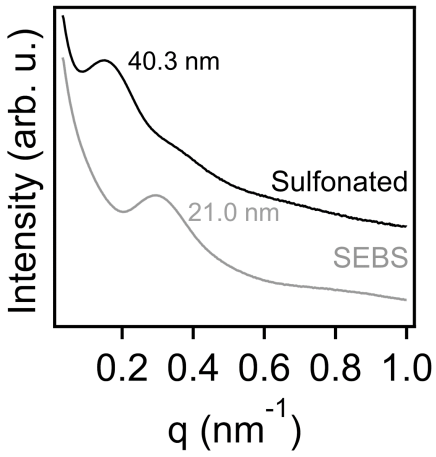

Figure S1. Small angle x-ray scattering (SAXS) results of neat SEBS and SEBS after sulfonation-induced crosslinking.

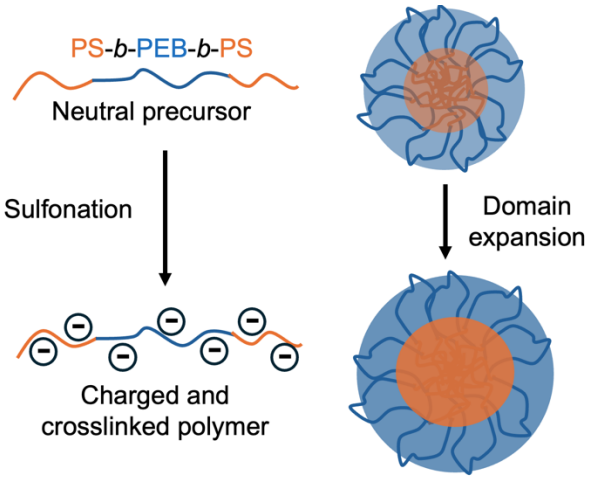

Scheme S1. Illustration of the effect of the sulfonation-induced crosslinking process on the nanostructure of the SEBS precursor.

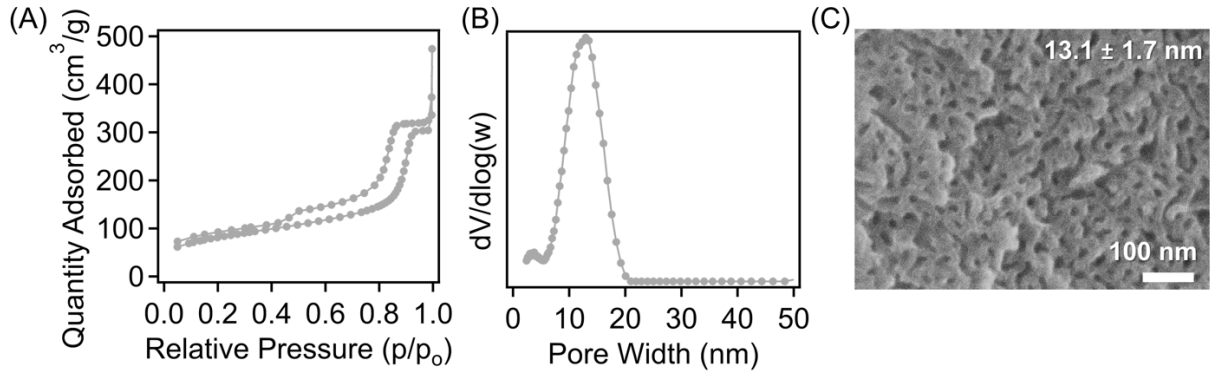

Figure S2. (A) Nitrogen physisorption isotherm, (B) NLDFT pore size distribution, and (C) SEM image of the OMCs prior to any functionalization.

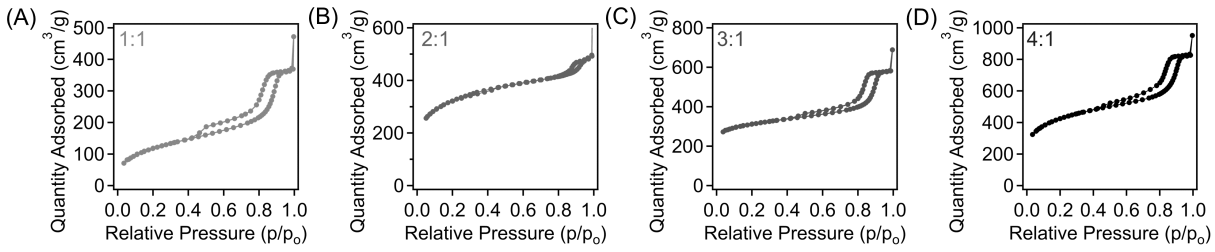

Figure S3. Nitrogen physisorption isotherms of SEBS-derived OMCs activated using KOH to carbon mass ratios of (A) 1:1, (B) 2:1, (C) 3:1, and (D) 4:1.

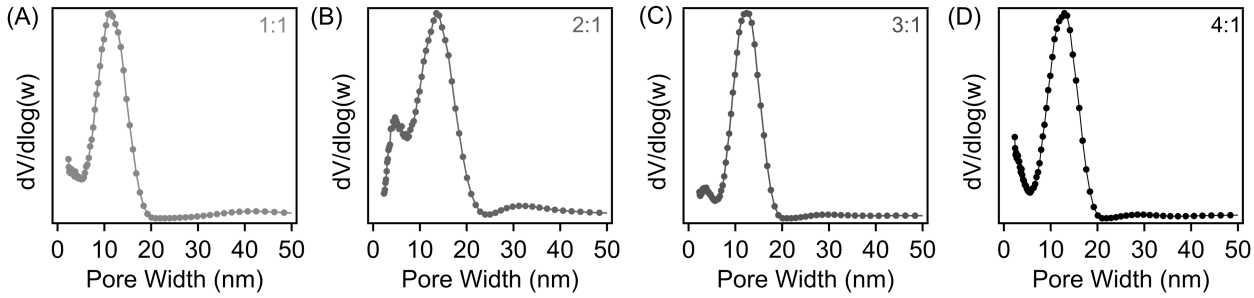

Figure S4. Nonlocal density functional theory (NLDFT) pore size distributions of the activated SEBS-OMCs calculated from the physisorption isotherms in Figure S3.

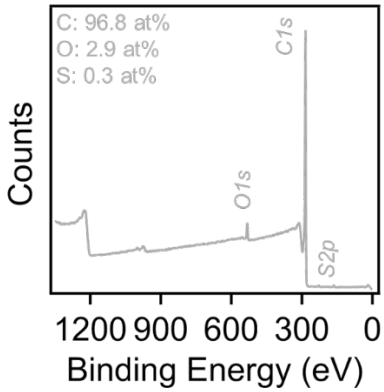

Figure S5. XPS survey scan for SEBS-derived OMC prior to functionalization.

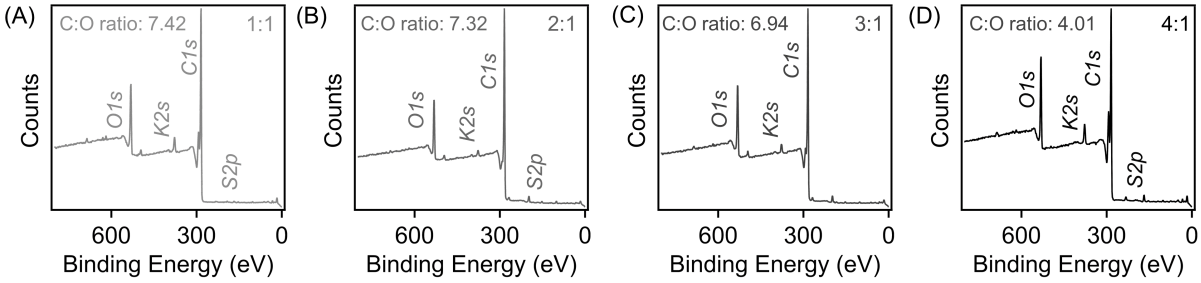

Figure S6. XPS survey scans of SEBS-derived OMCs activated using KOH to carbon mass ratios of (A) 1:1, (B) 2:1, (C) 3:1, and (D) 4:1.

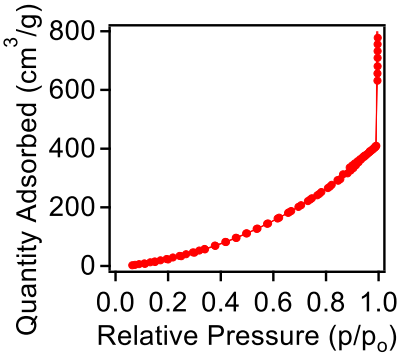

Figure S7. Liquid nitrogen physisorption isotherm of nitrogen-doped OMCs fabricated at a 1:1 mass ratio of melamine to mesoporous polymer exhibiting no hysteresis between the adsorption and desorption branches, indicating the absence of uniform mesopores.

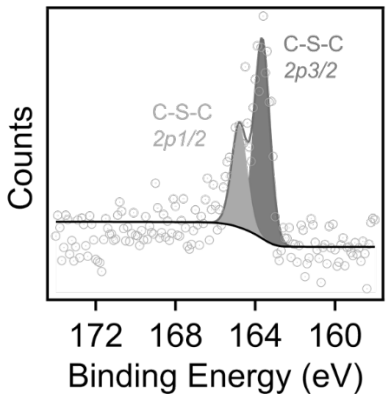

Figure S8. High resolution *S2p* scan for SEBS-derived OMC prior to functionalization.

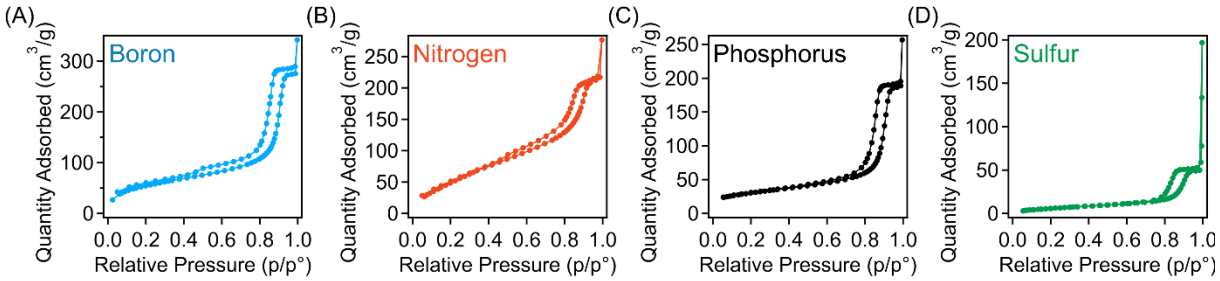

Figure S9. Nitrogen physisorption isotherms for (A) boron, (B) nitrogen, (C) phosphorus, and (D) sulfur doped carbons.

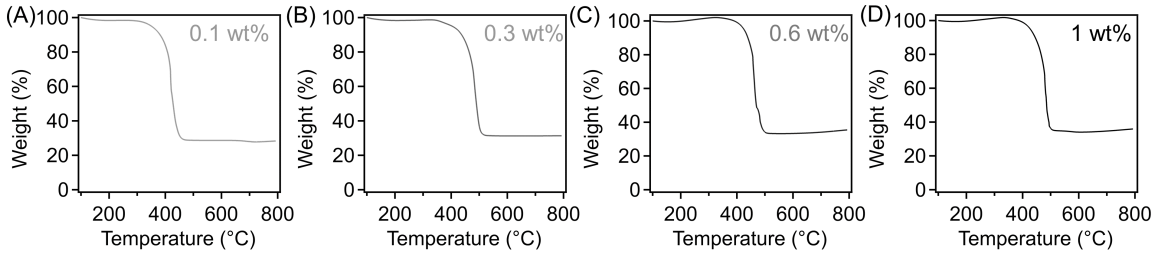

Figure S10. TGA results for calcium loaded carbons in air for samples which were loaded with metal nitrates from (A) 0.1wt%, (B) 0.3wt%, (C) 0.6wt%, and (D) 1wt% solutions of calcium nitrate.

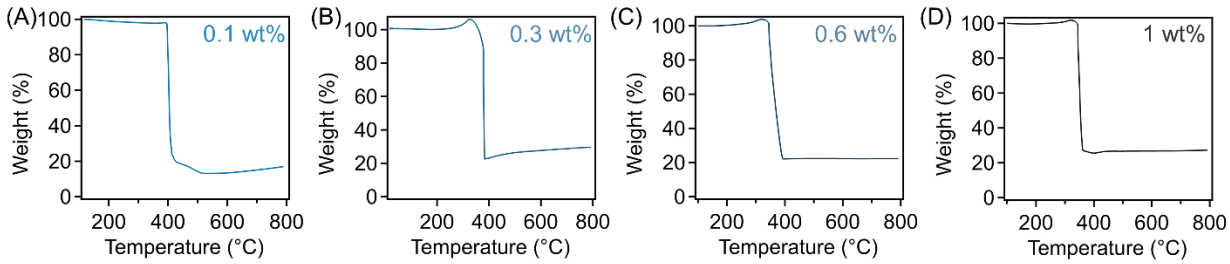

Figure S11. TGA results for copper loaded carbons in air for samples which were loaded with metal nitrates from (A) 0.1wt%, (B) 0.3wt%, (C) 0.6wt%, and (D) 1wt% solutions of copper nitrate.

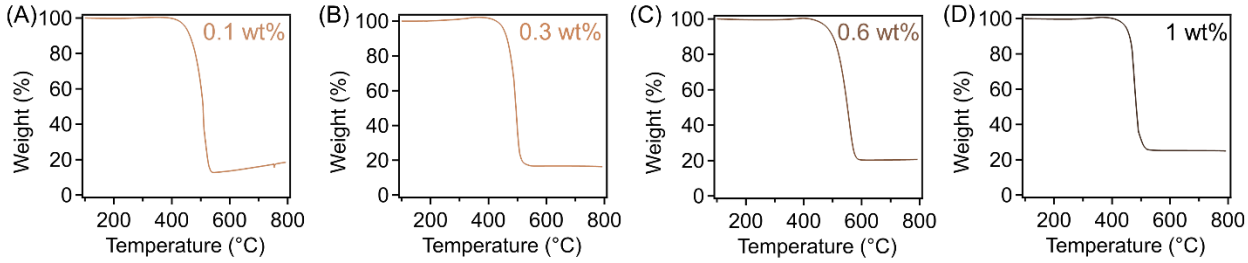

Figure S12. TGA results for nickel loaded carbons in air for samples which were loaded with metal nitrates from (A) 0.1wt%, (B) 0.3wt%, (C) 0.6wt%, and (D) 1wt% solutions of nickel nitrate.

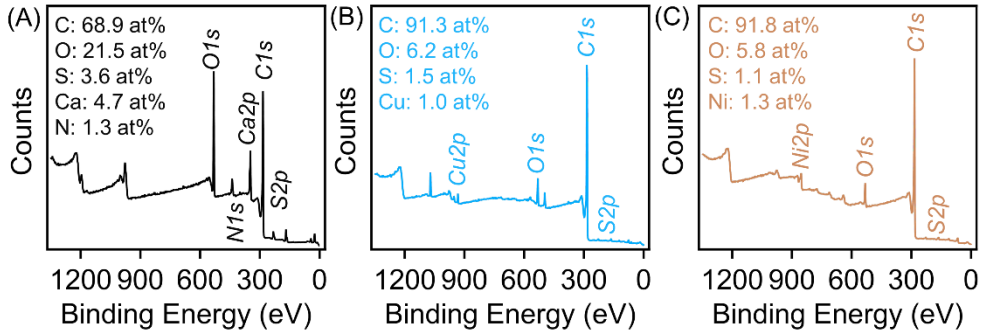

Figure S13. XPS survey scans of carbon loaded with (A) calcium, (B) copper, and (C) nickel from 0.1 wt% solutions.

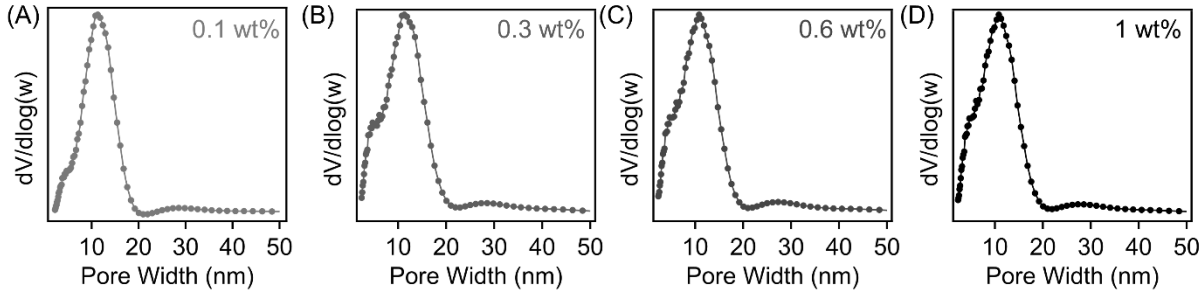

Figure S14. Pore size distributions for nanoparticle loaded OMCs prepared from calcium nitrate solutions of (A) 0.1 wt%, (B) 0.3 wt%, (C) 0.6 wt%, and (D) 1 wt%.

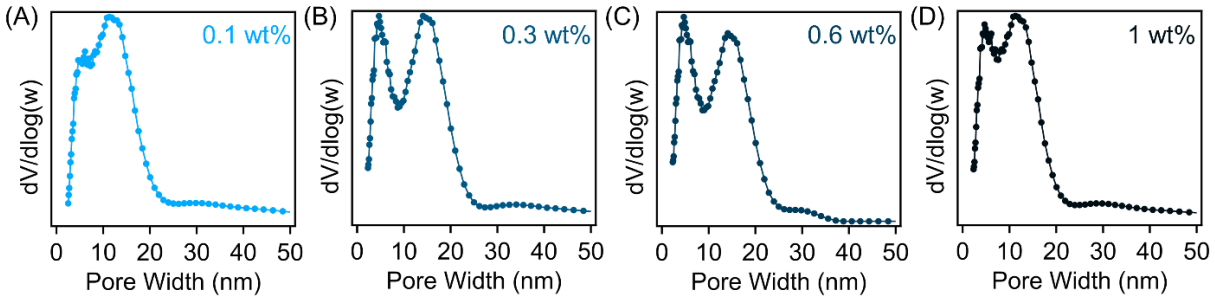

Figure S15. Pore size distributions for nanoparticle loaded OMCs prepared from copper nitrate solutions of (A) 0.1 wt%, (B) 0.3 wt%, (C) 0.6 wt%, and (D) 1 wt%.

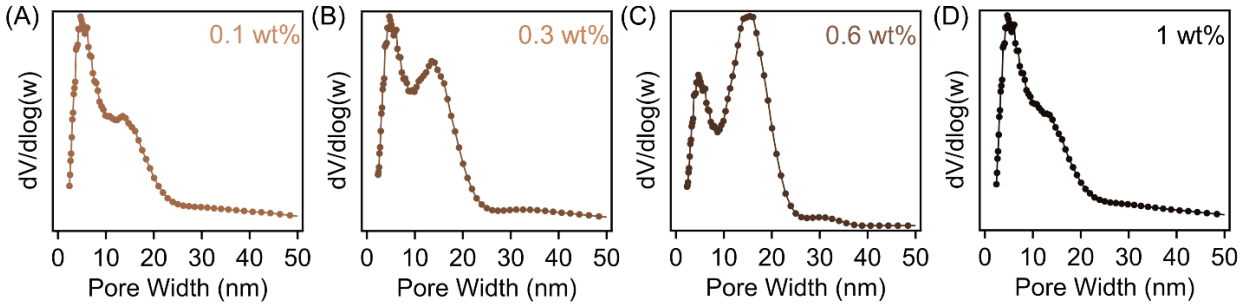

Figure S16. Pore size distributions for nanoparticle loaded OMCs prepared from nickel nitrate solutions of (A) 0.1 wt%, (B) 0.3 wt%, (C) 0.6 wt%, and (D) 1 wt%.

Table S1. Domain spacing results extracted from SAXS patterns of metal nanoparticle loaded samples depicted in Figure 9 in the main text.

	Domain Spacing (nm)		
Solution Concentration	Calcium	Copper	Nickel
0.1 wt%	27.8	30.7	30.3
0.3 wt%	29.1	29.9	29.9
0.6 wt%	29,1	29.1	31.6
1 wt%	31.2	29.9	29.9